

# Large-scale contraction of coronal loops and subsequent confined flux rope eruption during various phases of an M-class flare

Bhuwan Joshi<sup>1</sup>

**Collaborators:** Upendra Kushwaha<sup>1</sup>, Astrid Veronig<sup>2</sup>, and Y. J. Moon<sup>3</sup>

(1) Udaipur Solar Observatory, Physical Research Laboratory, Udaipur, India

(2) Kanzelhoehe Observatory/Institute of Physics, University of Graz, Graz, Austria

(3) School of Space Research, Kyung Hee University, Yongin, Gyeonggi-Do, Korea

# Solar Flares

---

- ❖ **Flares:** Transient, explosive perturbations in the solar atmosphere.  
(in excess of  $10^{32}$  erg)
- ❖ Two broad categories: **Confined** and **Eruptive**  
“Failed eruptions” – *a category of filament eruption*
- ❖ **Magnetic reconnection** has been recognized as the the fundamental process for the rapid conversion of stored magnetic energy into heat and kinetic energy of plasma and particles.
- ❖ **Particle acceleration:** Electrons and ions accelerated to high energies escape into the interplanetary space or remain trapped in the corona and chromosphere.
- ❖ **Thermal & non-thermal emissions:** Plasma of wide range of temperatures (cool plasma eruption observed in H $\alpha$  to a rapidly heated plasma in excess of 10 million K as recorded in X-rays); non-thermal particle (diagnosed in hard X-ray and radio): Multi-wavelength measurements are essential.

# Key components of a multi-wavelength flare

---

- ❑ Sigmoids
  
- ❑ Impulsive phase
  - Coronal emission, looptop sources
  - Footpoint sources, flare ribbons
  - Soft-hard-soft spectral evolution
  
- ❑ Gradual phase
  - Prolonged emission from hot coronal loops
  - Chromospheric evaporation
  - Neupert effect
  
- ❑ Cusp
  - Formation of cusp above the hottest outer loops
  
- ❑ Post-flare arcades

## Beyond “standard” observations

### ❑ Contraction of coronal loops

(Sui & Holman 2003, Veronig et al, 2006, Li & Gan 2006, Joshi et al. 2007, 2009, Simoes et al. 2013)

### ❑ Converging motion of footpoints

(Ji et al. 2006, 2007, Liu et al. 2009)

### ❑ Double coronal sources

(Sui & Holmann 2003, Liu et al 2008)



## Event

SOL2004-07-14

GOES class : M6.2

Active region : NOAA I0646

Location : N14 W61

Observing time : 04:30-06:00 UT

## Motivation

- ❖ To understand the phenomena of coronal implosion by combining EUV and X-ray, and MW data.
- ❖ To study temporal evolution of flare energies (thermal/non-thermal).
- ❖ How the confined eruption evolves?.

# OBSERVATIONS

- Observation of solar active region NOAA 10646 on 2004 July 14 from 4:00 – 6:00 UT.
  - M 6.2 flare and associated coronal activity

## Reuven Ramaty High Energy Solar Spectroscopic Imager (RHESSI)

RHESSI observes the full Sun with an unprecedented combination of spatial resolution (as fine as  $2''.3$ ) and energy resolution (1–5 keV) in the energy range of 3 keV to 17 MeV.

## Nobeyama Radio Heliograph (NoRH)

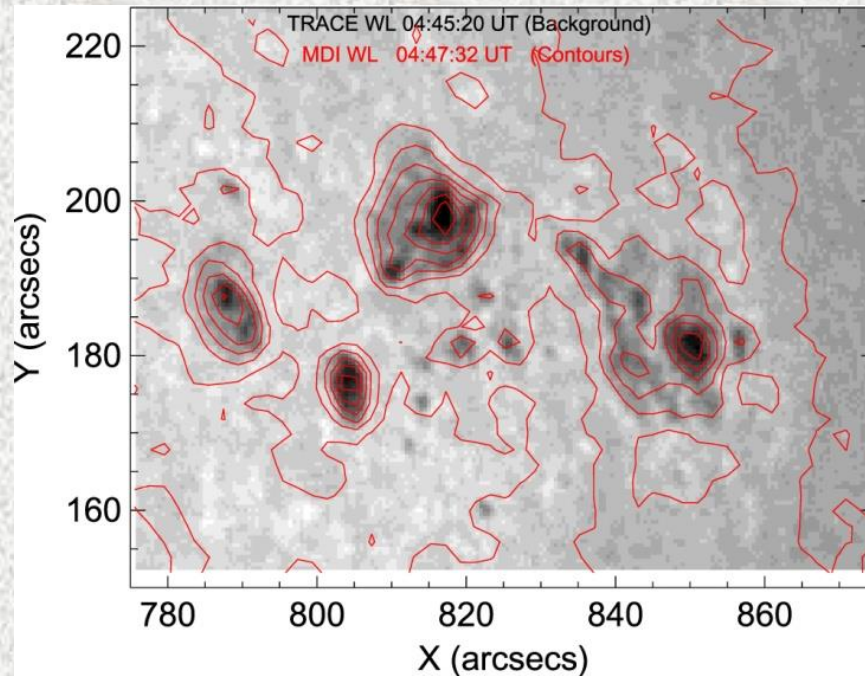
Solar Observations at 17 GHz and 34 GHz frequencies.

NoRH has a spatial resolution of  $10''$  and  $5''$  respectively. NoRH has a sensitivity of at least 1 solar flux unit (sfu) at 17 GHz and 3 sfu at 34 GHz

## Transition Region and Coronal Explorer (TRACE)

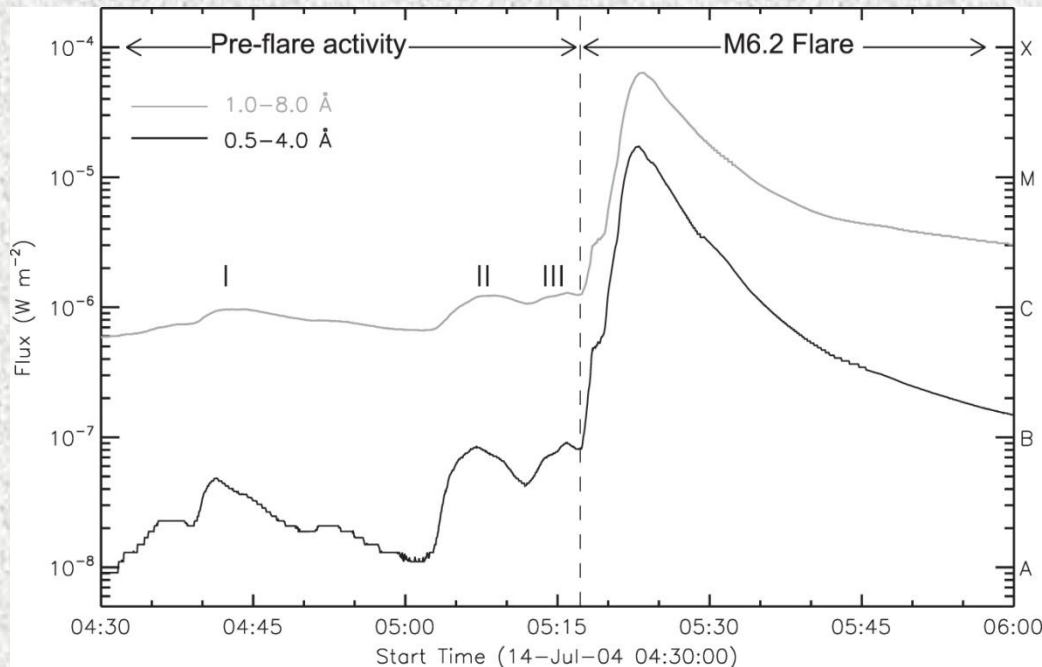
The TRACE telescope has a field of view of  $8.5 \times 8.5$  and a spatial resolution of 1 (0.5 pixel<sup>-1</sup>). The TRACE 171 Å filter is mainly sensitive to plasmas at a temperature around 1 MK (Fe IX)

# ALIGNMENT OF EUV AND X-RAY IMAGES



- ❑ Comparison of TRACE WL image and a SOHO WL image after alignment.
- ❑ For the cross-correlation, we used method of Gallagher et al. (2002).



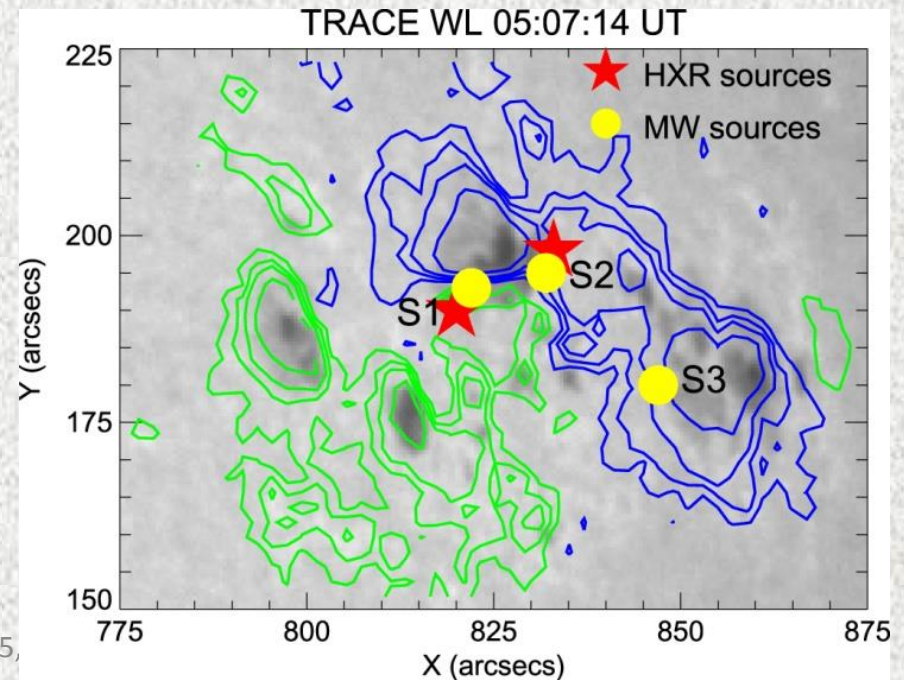
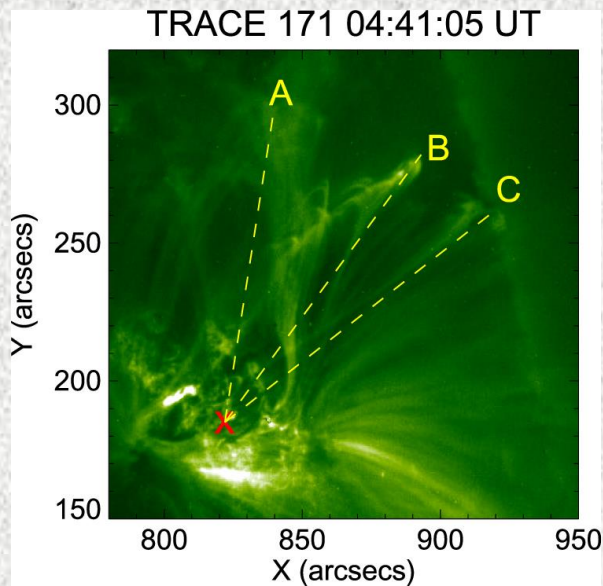


M6.2 flare: 05:17-06:00 UT  
 Pre-flare events at ~04:41 UT,  
 ~05:06 UT and ~05:16 UT

### ACTIVE REGION NOAA 10646

- ☐ Flare location N14 W61
- ☐ Leading sunspot groups: positive polarity
- Following sunspot groups: negative polarity
- ☐ HXR flare location: close to neutral line

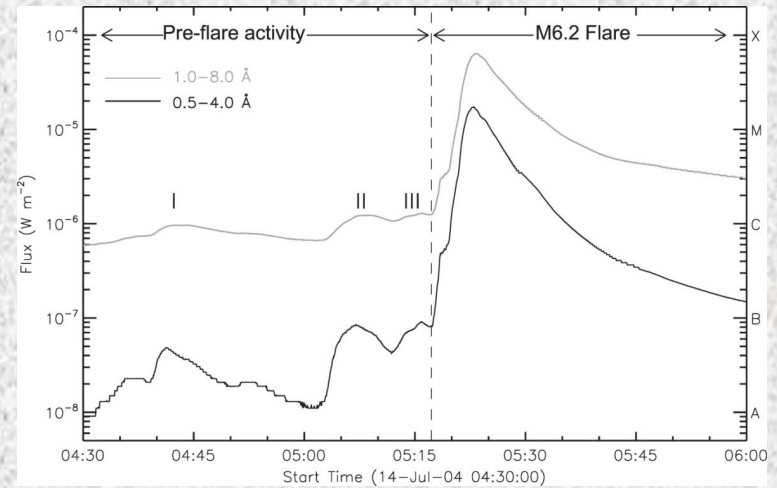
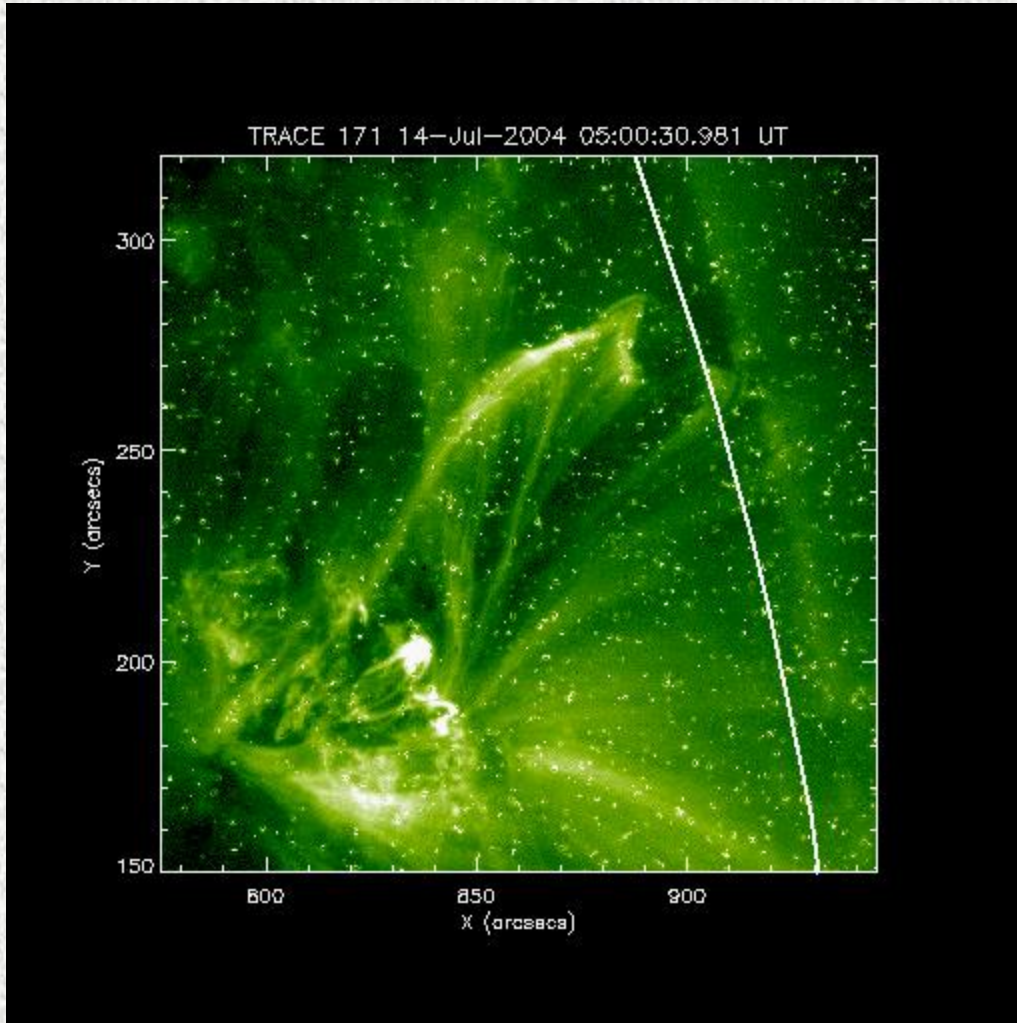
Positive: blue  
 Negative: green





# Pre-flare activity and M6.2 flare:

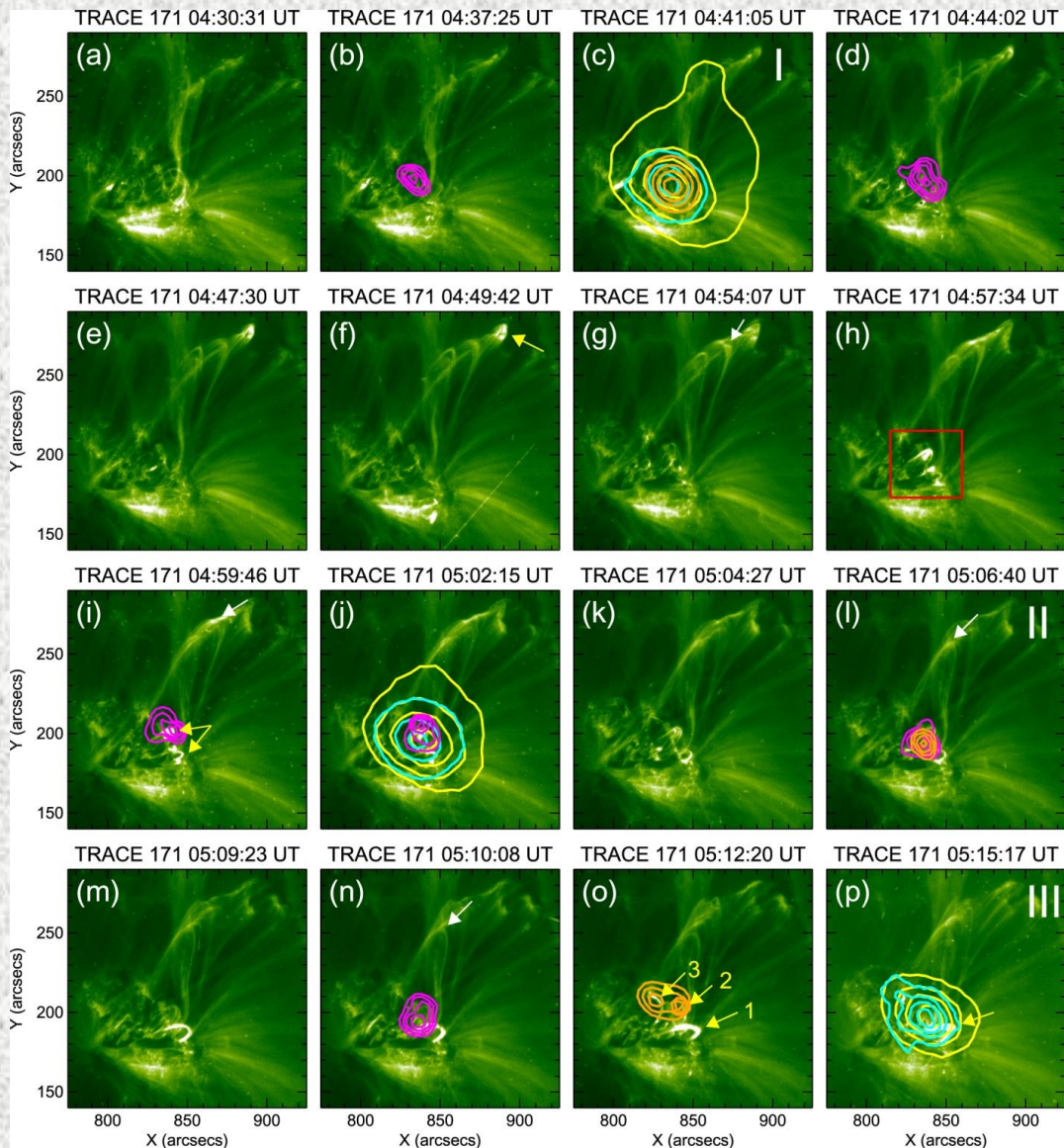
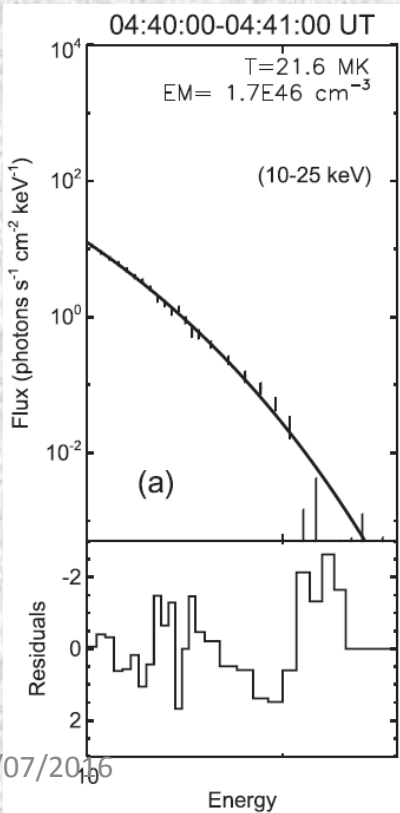
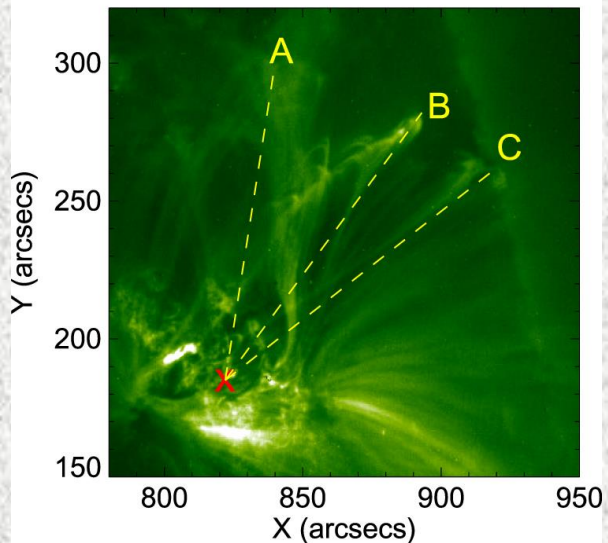
*Phases of implosion and expansion of coronal magnetic fields*



**Contraction** : 04:47 to 05:18 UT

**M6.2 flare** : 05:17 to 05:35 UT

# TRACE 171 04:41:05 UT



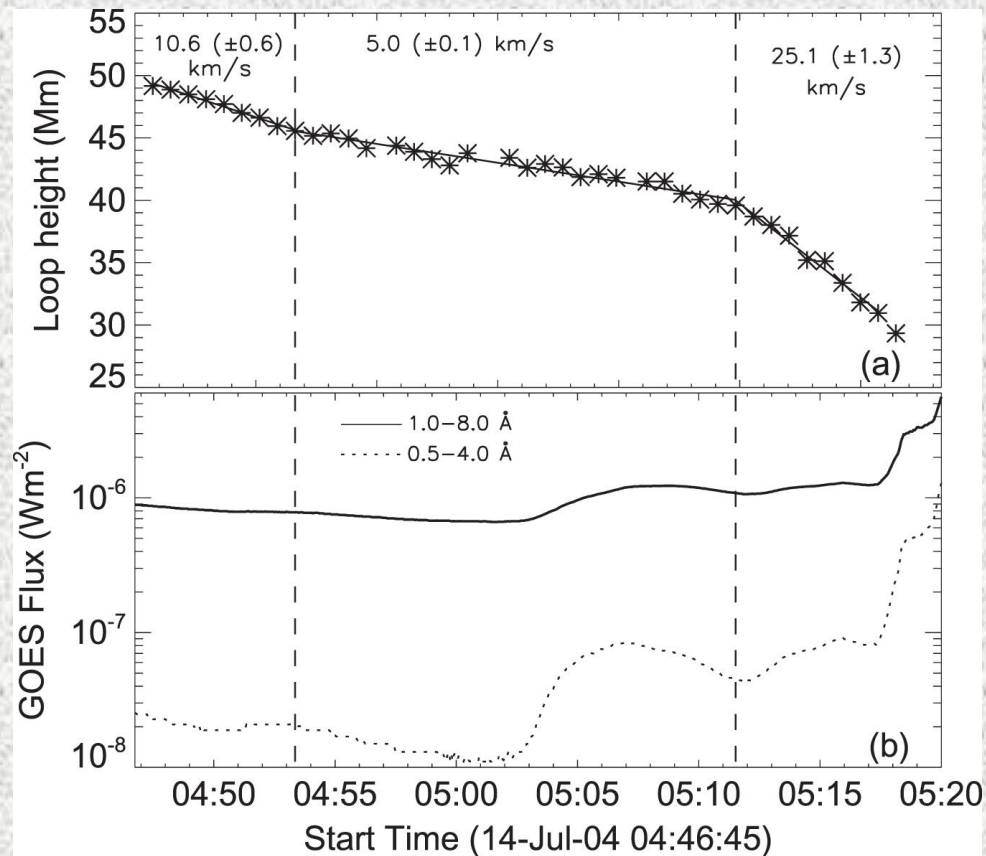
**RHESSI**

6–12 keV: magenta, 12–25 keV: orange

**NoRH**

17 GHz: yellow, 34 GHz: sky



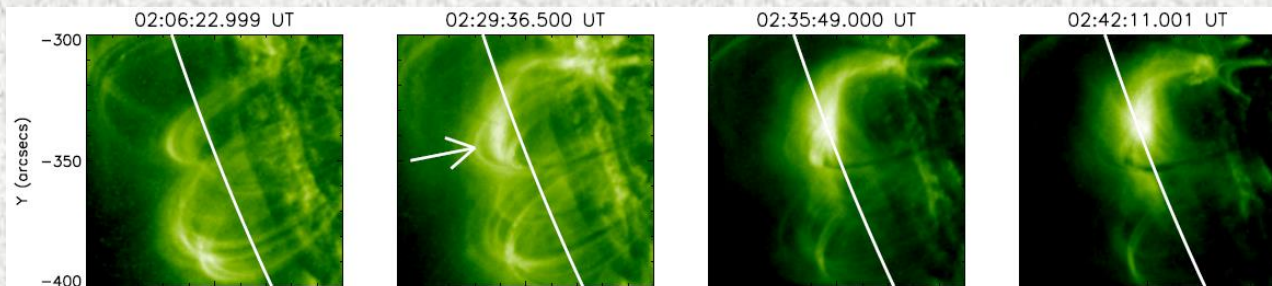
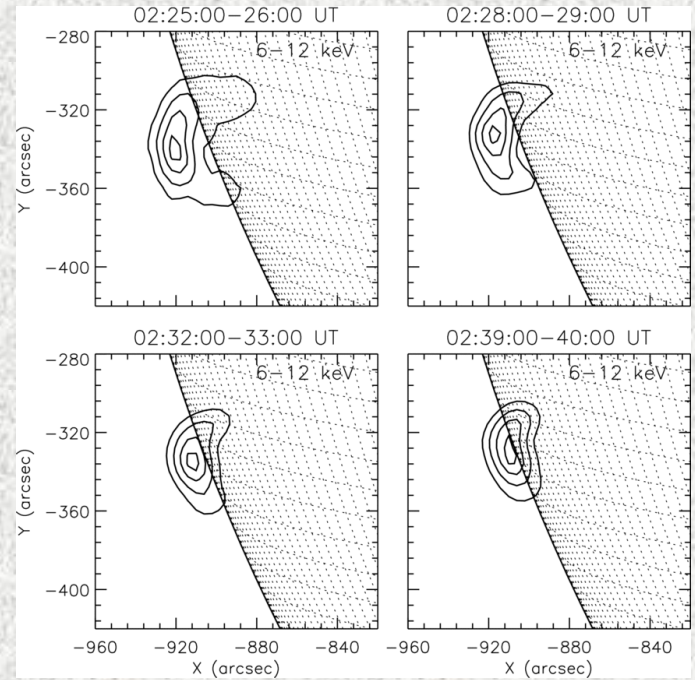
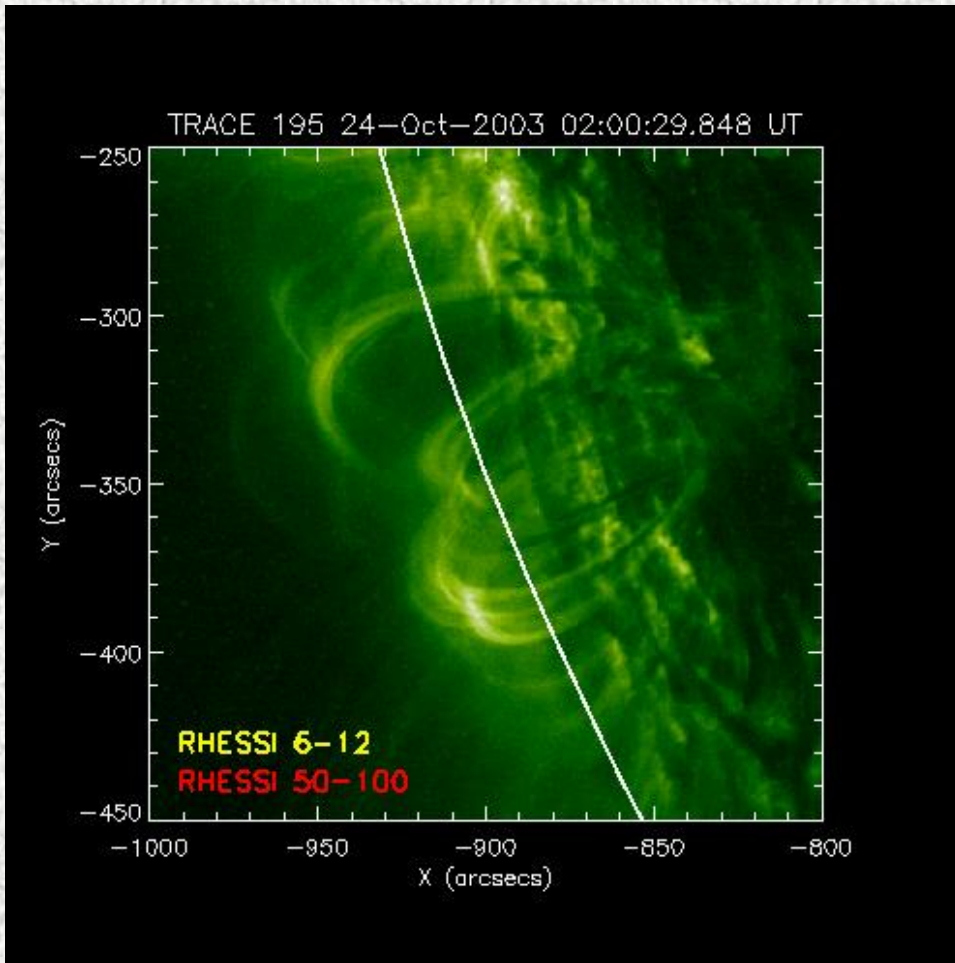


## Large-scale contraction of coronal loops

- ❑ Contraction proceeds for ~30 minutes during which overlying loops underwent contraction by 20Mm (~40% of their original height)
- ❑ EUV and X-ray emission from the core region; X-ray emission is predominantly thermal (~20 MK).
- ❑ The onset of the impulsive phase can be treated as the transition from inward to outward motion of coronal loops.

# SOL2003-10-24 M7.6

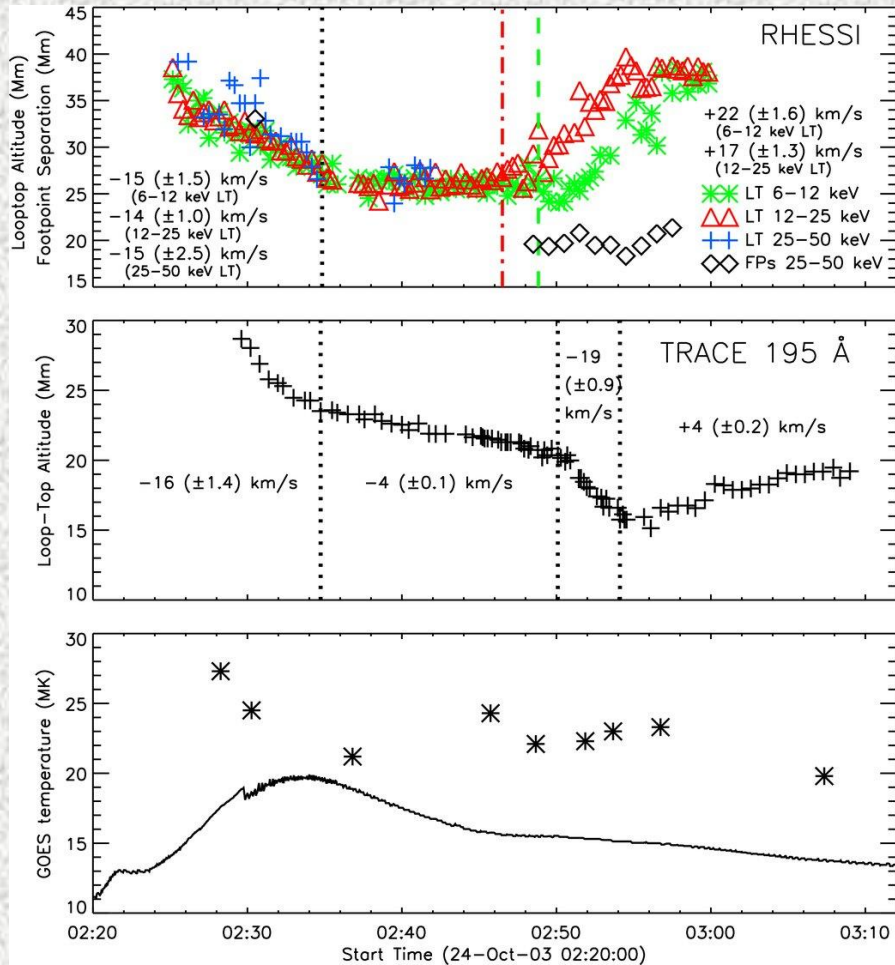
Joshi et al. 2009, ApJ, 706, 1438



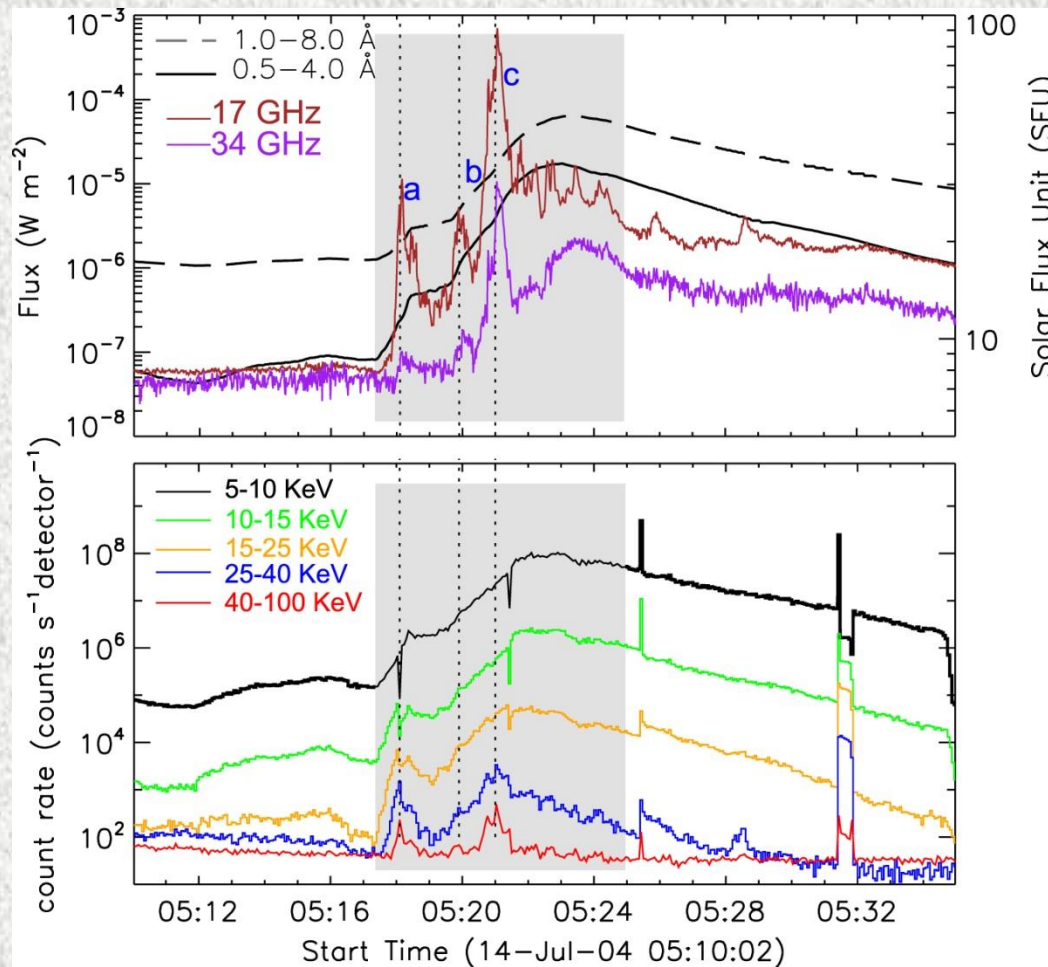


# SOL2003-10-24 M7.6

Joshi et al. 2009, ApJ, 706, I438

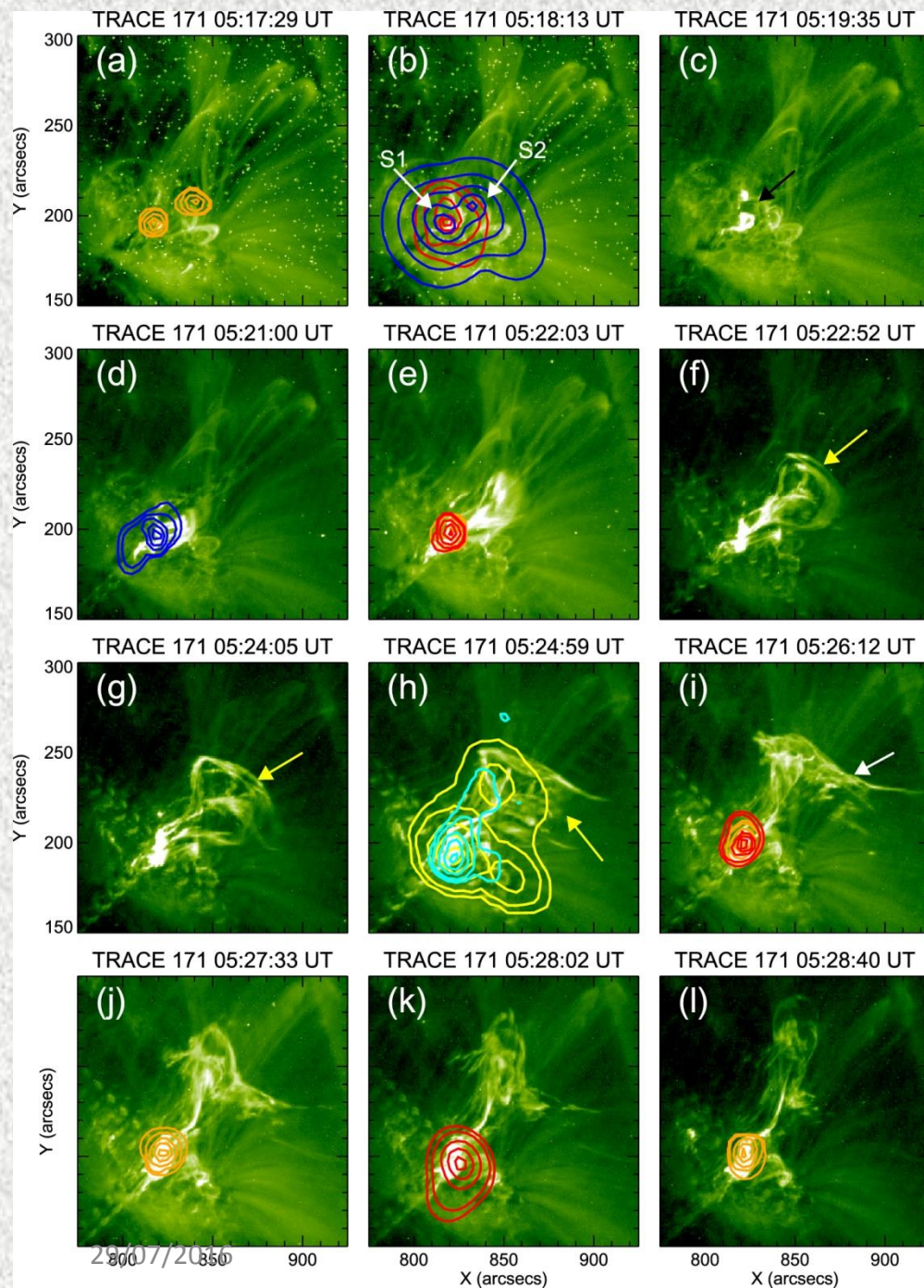


## M6.2 FLARE: X-RAY AND MW LIGHT CURVES



- ❑ Multiple (three) peaks during the impulsive phase
- ❑ Strong non-thermal emission during third peak



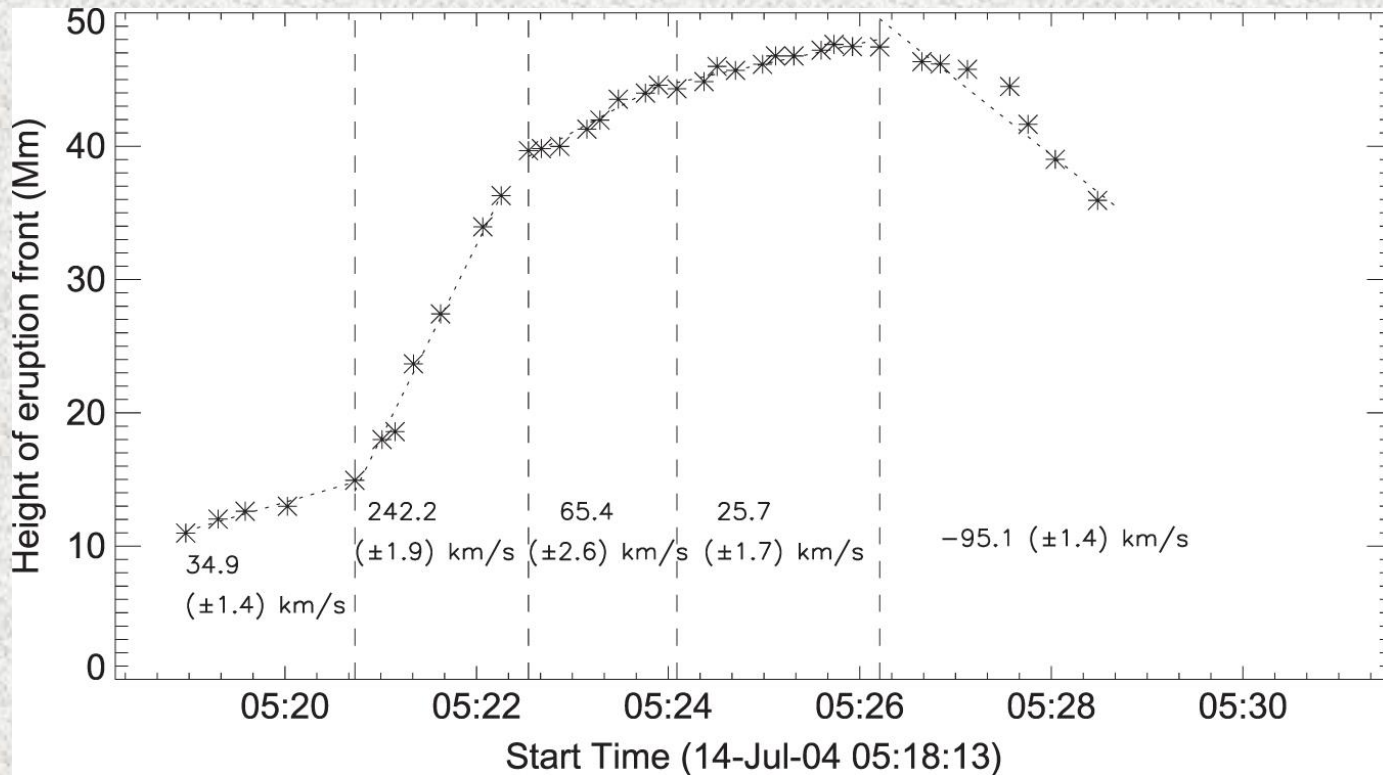


## M6.2 FLARE IMPULSIVE PHASE

- ☐ Initiation of eruption:  
*high energy HXR emission*
- ☐ Fast ejection of filament followed by its disruption.
- ☐ MW sources during the decay phase.

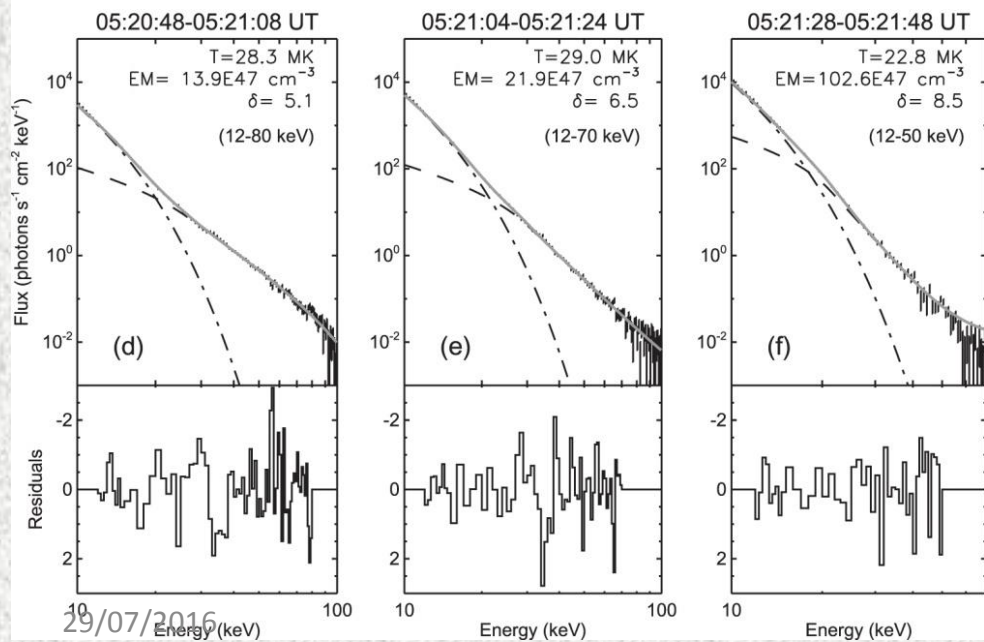
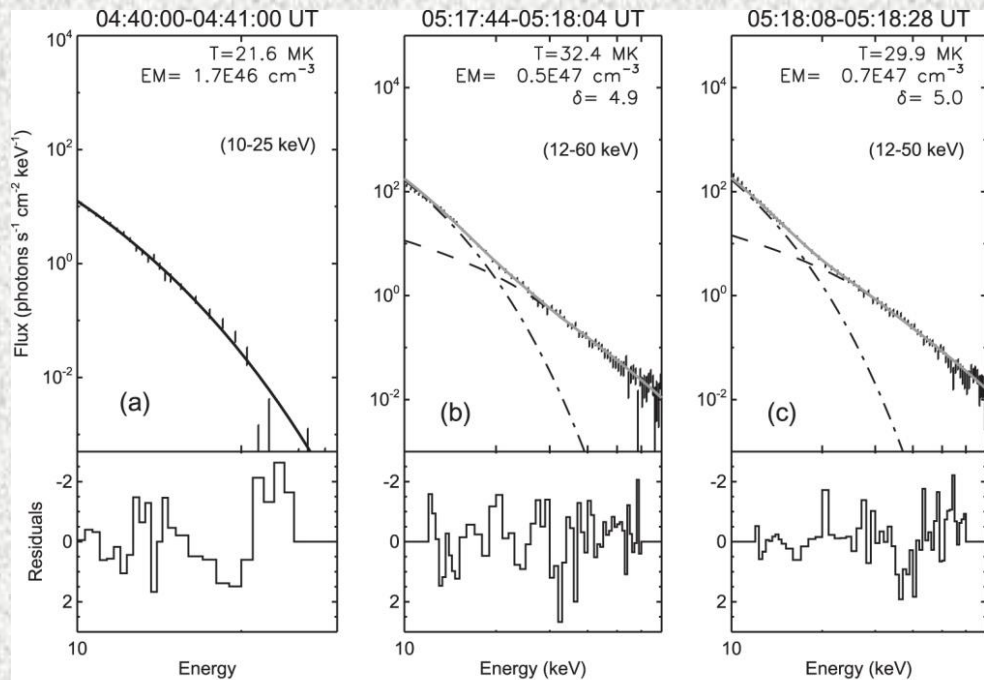
☐ **RHESSI images**  
 12–25 keV (orange)  
 25–40 keV (red)  
 40–100 keV keV (blue)

☐ **Nobeyama images**  
 17 GHz (yellow)  
 34 GHz (sky)

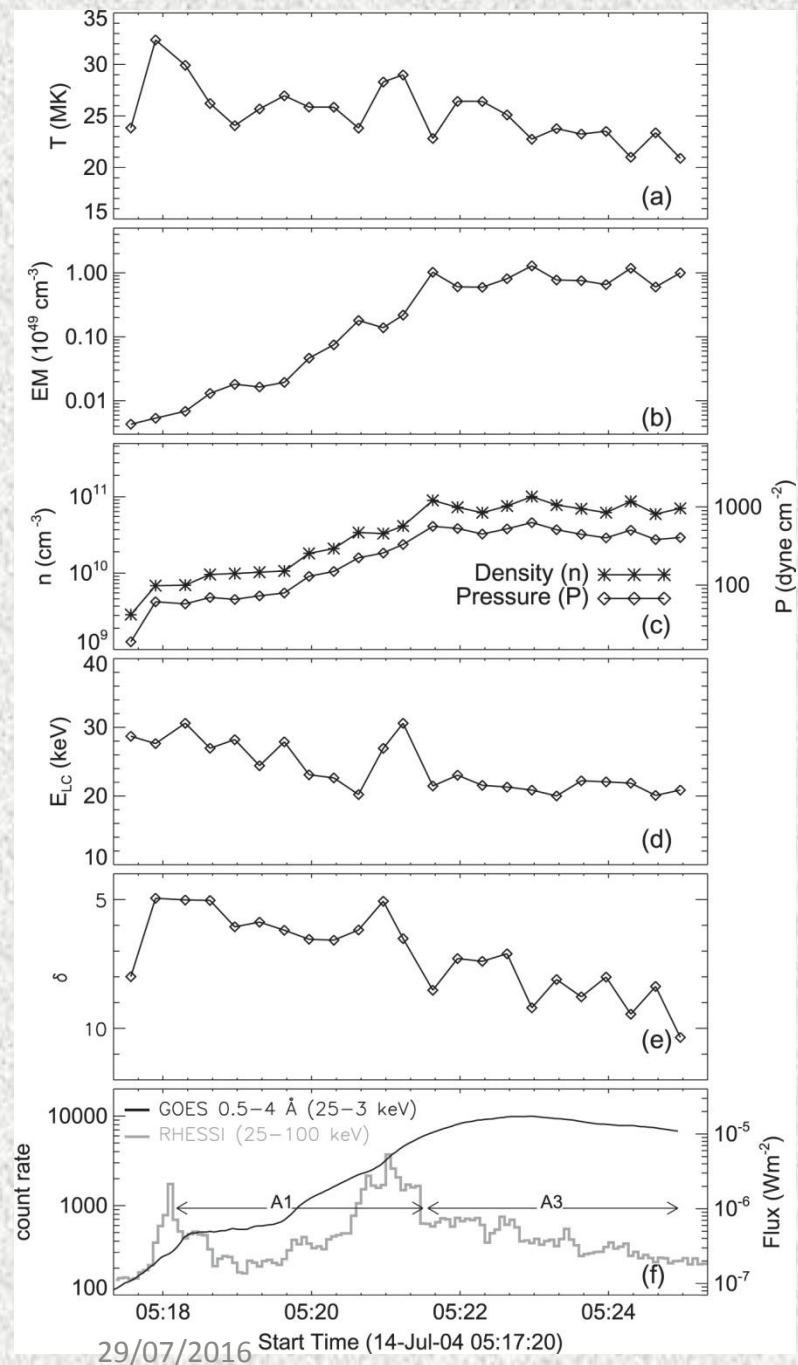


## Evolution of the prominence





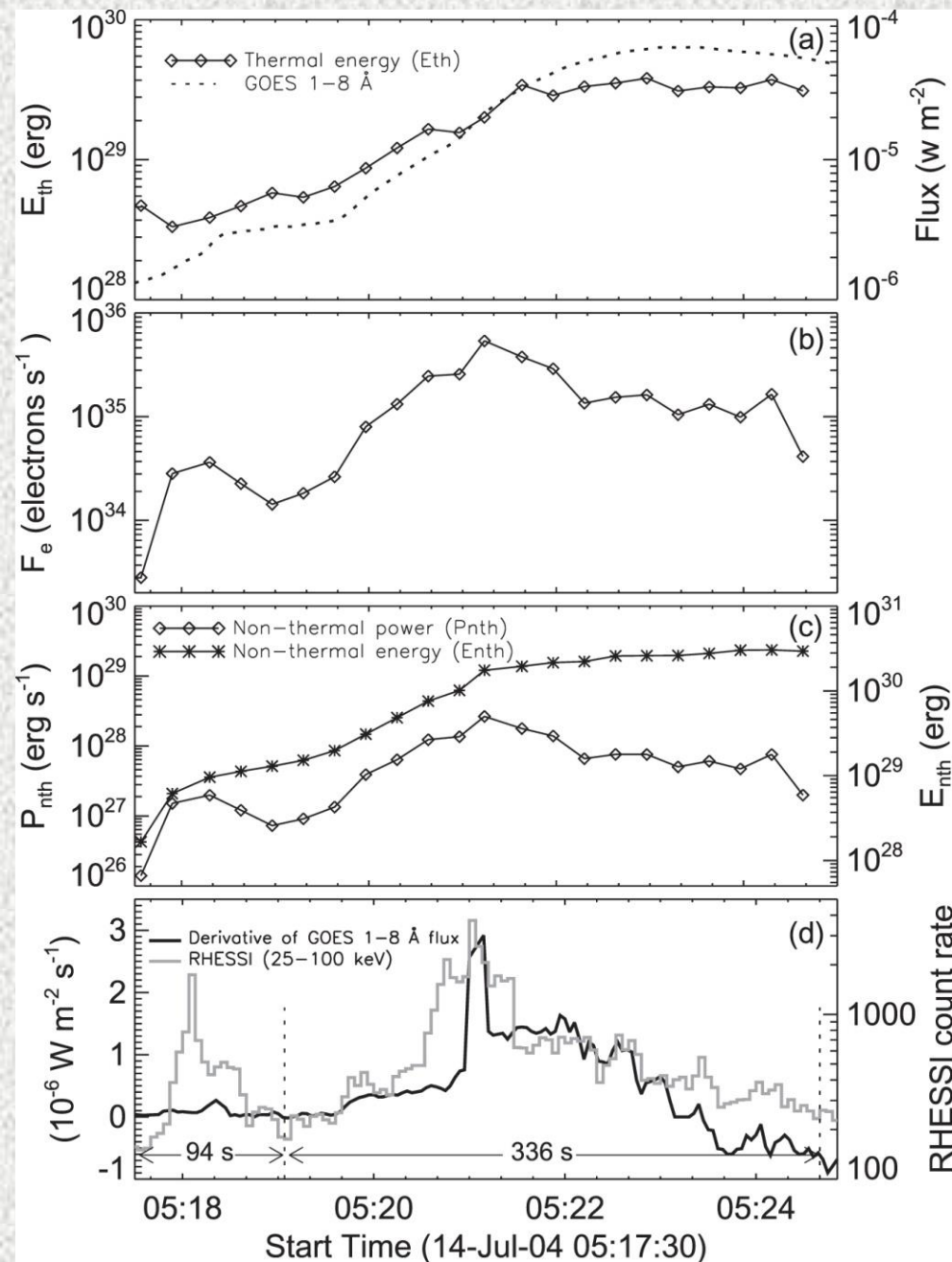
**Spectral fittings:**  
 Isothermal model (dashed-dotted)  
 Thick-target bremsstrahlung model (dashed line)



□ **Area of source:** Area within 50 % contour levels of 6-15 keV sources.

□ The derived  $E_{LC}$  values are the upper estimates due to the dominance of the hot thermal contribution, and thus yield lower limits to the number of non-thermal electrons and their energies.

□ Spectral hardening at the two HXR peaks ( $\sim 5$ ).



Flare characteristics	Parameters
Duration of HXR impulsive phase	430 s
No. of HXR peaks	2
Total non-thermal energy ( $(E_{nth})_{tot}$ )	$3.03 \times 10^{30}$ erg
Thermal energy ( $E_{th}$ )	
-Thermal energy ( $(E_{th})_{max}$ )	$3.89 \times 10^{29}$ erg
-Thermal energy ( $(E_{th})_{min}$ )	$0.33 \times 10^{29}$ erg
$(E_{nth})_{tot}/(E_{th})_{max}$	$\sim 7.5$

$$E_{th} = 3k_B T n V = 3k_B T \sqrt{EM \cdot f \cdot V} \text{ [erg]}$$

$$P_{nth}(E > E_{LC}) = \frac{\delta - 1}{\delta - 2} F_e E_{LC} 10^{35} \text{ [erg s}^{-1}\text{]}$$

$E_{LC}$  : low-energy cutoff (varies 20-32 keV)  
(fixed at average value of 25 keV)

$F_e$  : total no. of electrons above  $E_{LC}$



# Summary

- We report large-scale implosion of overlying coronal loops that continued over 30 minutes during which overlying loops underwent contraction by 20 Mm ( $\sim 40\%$  of their original height) during the pre-flare phase. Such a large-scale contraction has been reported for the first time.
  - Simultaneous to the loop contraction, episodic and localized events of energy release occurred in low-lying loops at the core of the large overlying loops. Prolonged loop contraction as a manifestation of localized and intermittent events of energy release during the pre-flare phase (Hudson's conjecture; Hudson 2000).
  - Plasma was already substantially preheated at the flare core before the onset of impulsive phase. Strong preheating at the flare core will contribute favorably to efficient particle acceleration during the subsequent impulsive phase of the event.
  - The flux rope activated during the impulsive phase but could not have a successful escape through the overlying coronal loops and therefore leads to a confined eruption (i.e., no CME).
  - The time evolution of thermal energy nicely correlates with the variations of the cumulative nonthermal energy throughout the impulsive phase of the flare. This can be interpreted in terms of efficient conversion of the energy of accelerated particles to hot flare plasma and is well consistent with the Neupert effect.
- Kushwaha, Upendra, Joshi, Bhuwan, Veronig, Astrid, & Moon, Yong-Jae, 2015, ApJ, 807, 101
  - Joshi, Bhuwan, Veronig, Astrid, Cho, K.-S, et al. 2009, ApJ, 706, 1438-1450.